 doi:10.20944/preprints201805.0282.v1

Article

Influence of Single Fracture Inclination on Fault Activation

Yujie Zhu [1], Xiaoli Liu [1*], Enzhi Wang [1], Sijing Wang [1], Jianwen Zhong [1]

[1] State Key Laboratory of Hydro-Science and Engineering, Tsinghua University, Beijing 100084,China; zhu-yj16@mails.tsinghua.edu.cn (Y.Z.); nzwang@tsinghua.edu.cn (E.W.)

* Correspondence: xiaoli.liu@tsinghua.edu.cn; Tel.: +86-10-6279-4910; Fax: +86-10-6278-2159

Abstract: Pre-existing fracture and secondary cracks in rock mass are formed by natural power, such as magma condensed to igneous rocks and tectonic movement. The orientation and inclination of these fractures obey certain laws relating to the stress, temperature, minerals, water and so on. Therefore, cracks react differently under the same external loading on the condition of various inclination, fissure apertures, stiffness and joint roughness. To simulate the crack propagation, experiments on hollow cylinder cut by one oblique interface mimicking single fracture accumulated numerous data discovering the failure criterion in accordance with the Mohr-Coulomb criterion. And theory on the Terzaghi's effective principle take an essential role in controlling the behavior of triggering fault. This paper introduced a series of oblique plane cutting the cylinder regarded as fractures at different inclination to concentrate on how the fracture characteristic effect the stress and strain distribution inside the specimen, especially, the relationship between displacement and water head. The key point of this numerical simulation is coupling the solid phase and the fluid phase, specifically, the mechanic and seepage field. According to the statics, curves referring to deformation and water head could be described as increasing lines. Besides, simulation on coupling solid phase and fluid phase can supply crucial evaluation on activating existing fault, and thus predicting induced seismicity in reservoirs or estimating damage in shale gas exploration.

Keywords: Hydraulic fracturing; hollow cylinder; single fracture; fault activation; induced seismicity

1 Introduction

Hydraulic-fracturing is related to many engineering construction such as the excavation of shale gas and enhanced geothermal system, defined as a physic phenomenon that cracks in soil and rocks generate and develop under the condition of sharp soar of water pressure.(Huang Wenxi, 1982) However, damage induced by mechanical or hydraulic perturbations would not only influence the permeability of the rock mass, but also effect the pore pressure distribution.(Maria Laura De Bellis, 2017) When the water pressure in a well suddenly changes, the pore pressure in the rock mass around the well would get modification subsequently. Therefore, the physic and mechanic characters of rock mass would response to the coupling process. (Kranz, 1983; Wong et al., 1996) However, when the external load is substituted from static force into dynamic force, the mechanism of generating cracks would be different. This phenomenon might explain the core mechanism of the crack generation and extension in rock mass under the condition of reservoir induced seismicity.

Many researchers have done indoor and outdoor hydraulic fracturing experiments, especially the indoor experiences, for its advances in explicit boundary conditions and easy control. In 1972, Bjerrum and Andersen simulated the hydraulic fracturing in conventional triaxial test device, applying the water pressure in a pipe inserted in a rock cylinder. The result indicated that the fractures closure pressure was equal to the confining pressure while the cleavage plane was perpendicular and extended to the edge.(Bjerrum, 1972; Zhang Hui, 2005) Afterwards, experiments revealed one necessary condition of hydraulic fracturing was the minimum principle stress reaching the tension stress. (Nobari, 1973; Yaping Sun, 1985) Otherwise, Decker and Clemence pointed out that shear failure is the main damage of specimen, similar to Mohr-Coulomb failure criteria.(Decker, 1981) Since hydraulic fracturing is widely applied for gas exploration and enhanced geothermal system, it is an essential utility that create new hydraulic fractures and improve the connectivity of pre-existing natural fractures. (Saipeng Huang, 2017) Thus the direction and development of generating cracks would be influenced by the local stress distribution, which attracted many researchers investigating extensively. (Jaeger, 1979; Charlez, 1985; Brudy, 1999; Nelson, 2005; Ameen, 2014)

During this period, theories of hydraulic fracturing were also developing fast, according to the mechanics of materials, elastic mechanics, etc. The indoor experiments usually adopt hollow cylinder as specimens for its convenience in controlling the size and boundary conditions. Therefore this model is introduced into calculating the mechanic analytic solution, similar to the thick-wall cylinder in elastic mechanism. (L. C. Auton, 2017) When studying hydraulic fracturing, researchers assumed the specimen was an elastic material, which would be perfectly consist with the theory of elastic mechanism. (P. Grassl, 2015) However, the constitutive model would be related to the properties of specimen. Therefore the Mohr-Coulomb model would be consistent to the damage path in some experiments. (Decker, 1981) Apart from this, not only the damage mechanism (Maria Laura De Bellis, 2017; Xiaoxi, Men, Chunan Tang, 2013) but also the dynamic conditions (Chen, W. , Ravichandran, G. , 1996) were also considered into explaining the phenomenon of hydraulic fracturing.

At the end of the last century, simulations about fracturing process and propagation have been achieved for the rapid development of computer technologies. (Moes et al., 1999; Beekman et al., 2000; Li and Wong, 2012; Yao, 2012; Kim and Moridis, 2015) Many analysis methods were utilized in resolving problems in hydraulic fracturing, such as the finite element method, discrete element method and element-free method and so on. A number of 2D and 3D models were established to trace the pressure distribution and fluid flow in the fractures by Cleary and Wong (1985). Sousani simulated the fluid-solid coupling among discontinues materials such as joints, fractures and faults in sandstone or limestone by DEM (Discrete Element Method). (Sousani Marina, 2014) Wei Wu simulated the unloading-induced fault instability by using Particle Flow Code (PFC), experimentally examining the effects of initial shear stress and normal stress on assumed granular fault. (Wei Wu, 2017)

Previous works about the hydraulic fracturing were mainly focused on existing fault instability inside specimens under a wide range of confining pressure. Few simulation and experiments concentrate on the characteristics such as thickness, angles and stiffness of the fault. Inhomogeneous

 doi:10.20944/preprints201805.0282.v1

medium is quite different for the complication in mechanic field and seepage field. Discontinuity in rock mass is a crucial factor activating fault, releasing energy in the form of seismicity. However, seismicity may induce significant change in seepage and initial state, altering the crack extension expressed in static condition. In this article, we will discuss deformation of specimen with different interface under different water pressure, and mechanism of hydraulic fracturing while faults or other discontinues structure exist in rock mass.

2. Hydro-mechanical Models

Water and other substances may be contained in the fractures and pores of rock mass, forming a unity and performing as an integral. Therefore, the interaction of fluid and solid phases affects the quality and characteristics of rock. Especially in saturated rocks, the stress and strain would be totally different from the dry rocks. Deterioration of mechanical and hydraulic properties of rock masses and subsequent problems are closely related to changes in the stress state, formation of new cracks and increase of permeability in porous media saturated with freely moving fluids.

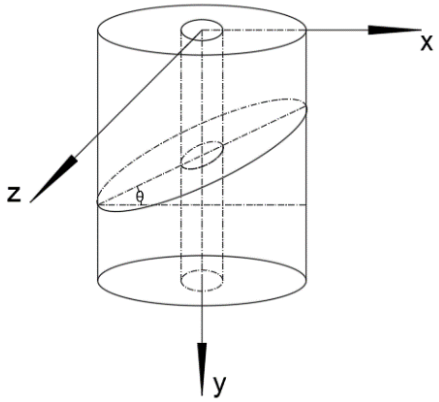

Figure 1. Model of hollow cylinder with an oblique plane.

Most experiments whatever practical tests or numerical simulations would choose hollow cylinder usually defined as thick-wall cylinder. The fluid would be injected in the hole and radically flow in the porous media along the radius. However, anisotropy is common since the fractures hiding in rocks, hard to be seen and described accurately by scientific technologies for now. Therefore when the fractures or cracks are settled inside the specimen, the model would be more complicated than the thick-wall cylinder. The formulas are in the following.

To explicitly describe the model, a circle with a hole is established in x-z plane, and extruded in y axis (Figure 1). The geometry in x-z plane could be regarded as thick wall cylinder while the cylinder is cut by an oblique plane perpendicular to the x-y plane. The angle between the oblique plane and x-z plane isθ.

Preprints (www.preprints.org) | NOT PEER-REVIEWED | Posted: 22 May 2018 doi:10.20944/preprints201805.0282.v1

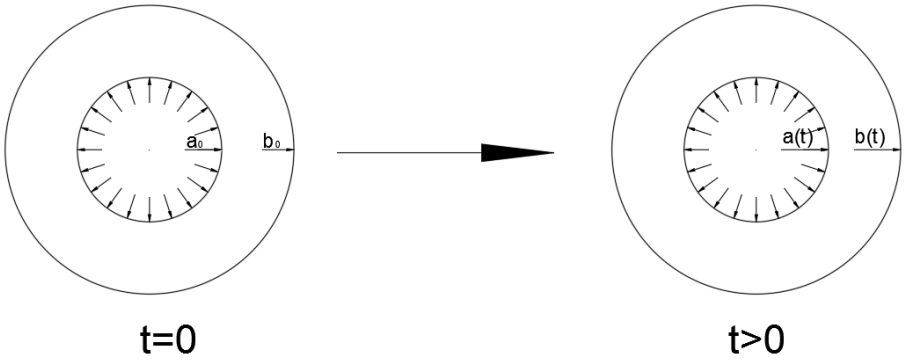

Figure 2. Fluid flow radially outward in x-z plane, and the inner radius is free to expand while the displacement of outer boundary is constrained.

Assuming a material is constrained in an axial direction with a center of porous cylinder of inner radius a and outer radius b. If the cylinder is homogeneous, this model would be regarded as a plane strain problem. The inner radius a=a(t) expands while the water pressure increases for the free inner boundary. And the outer radius $b(t)=b_0$ is fixed because the outer boundary is constrained.

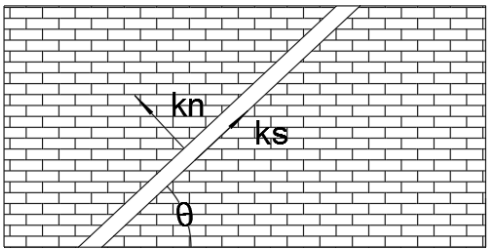

Figure 3. Interface in cylinder cut by fracture of which the friction, normal stiffness and shear stiffness should be assured. The angle between interface and x-z plane is θ.

As for the fractures in specimen, assuming they are perpendicular to x-y plane, the stress and strain would be much complicated for the sophistication in interface, whatever in the physic and mechanic characteristics in material or the permeability in fluid flow.

2.1. Kinematic equation

In the solid part, a micro cube is selected randomly. Its velocity v_s and displacement u_s each are related to the time t and its position r (radial coordinate r). Therefore, v_s and u_s could be expressed in the following:

$$\mathbf{u}_s = u_s(\mathrm{r},\mathrm{t})\hat{\mathbf{e}}_r \qquad \mathbf{v}_s = v_s(\mathrm{r},\mathrm{t})\hat{\mathbf{e}}_r \tag{2.1}$$

The displacement u_s is given in Eulerian reference framework.

$$u_s(\mathrm{r},\mathrm{t}) = \mathrm{r} - \mathrm{R}(\mathrm{r},\mathrm{t}) \qquad \frac{u_s}{r} = 1 - \frac{\mathrm{R}(\mathrm{r},\mathrm{t})}{r} \tag{2.2}$$

While t=0, the initial $u_s(\mathrm{r},0) = 0$ for the $\mathrm{R}(\mathrm{r},0) = \mathrm{r}$.

The strain ε_{rr} and $\varepsilon_{\theta\theta}$ are the radial and azimuthal components of the strain, which is two dimensional while the displacement is indeed one dimensional.

$$\varepsilon_{rr} = \frac{\partial u_r}{\partial r} \qquad \varepsilon_{\theta\theta} = \frac{u_r}{r} \tag{2.3}$$

In Lagrange framework, the deformation gradient tensor is defined as $\mathbf{F}=\frac{\partial x}{\partial X}$, where the x means displacement of the point and X is the position. Thus in Eulerian framework the deformation gradient tensor would be altered into $\mathbf{F}=(\mathbf{I}-\nabla\mathbf{u_s})^{-1}$ ($\mathbf{I}$ denotes the identity tensor and $(\cdot)^{-1}$ the inverse) (L. C. Auton, 2017), which can be written as following due to the thick wall cylinder is regarded as plane strain problem

$$F=\begin{pmatrix}\lambda_r & 0 & 0\\ 0 & \lambda_\theta & 0\\ 0 & 0 & \lambda_y\end{pmatrix} \tag{2.4}$$

λ_i^2 is the eigenvalue of $\mathbf{FF}^T$, in which the T means transpose, on the behalf of the square of principle stretch ratios, the λ_i could be decomposed as

$$\lambda_r=(1-\varepsilon_{rr})^{-1}\quad \lambda_\theta=(1-\varepsilon_{\theta\theta})^{-1}\quad \lambda_y=1 \tag{2.5}$$

The Jacobian determinant J could measure the local volume change. The formula is $J=\det(\mathrm{F})$, which could be $J=\lambda_r\lambda_\theta\lambda_y$.

However, an oblique plane cutting the cylinder would alter the values in deformation gradient tensor since the absence of unique axisymmetric character and discontinuity of materials after inserting an interface. On the contrary, the expression of $\mathbf{F}$ is the same, with six independent parameters.

2.2. Continuity equation

We hypothesize that the fluid of which viscosity is μ could not be compressed. All the deformation is caused by the rearrangement of solid skeleton while the pore pressure increases or decreases. According to the Bernoulli's principle, total hydraulic head h could measure the energy of permeability for slow flowing fluids in porous media.

$$h=\frac{p}{\rho_f g}+z \tag{2.6}$$

ρ_f is fluid density and g is gravitational acceleration. A piezometer can measure the value of $p/\rho_f g$. Besides z represents the position potential energy.(Maria Laura De Bellis, Gabriele Della Vecchia, Michael Ortiz, etc. , 2017)

We hypothesize that the permeability in porous media is accordant with the Darcy's law, namely denoting that the Reynolds number is less than 10. Afterwards the quantity of flow Q proportional to hydraulic head gradient $\mathbf{L}$.

$$Q=-\mathbf{K}\frac{\rho_f g}{\mu}\mathbf{L} \tag{2.7}$$

$\mathbf{K}$ is the material permeability tensor, describing the seepage on the condition of anisotropic, symmetric and positive for the reason that fluid cannot flow against pressure drop(Biot, 1972; Katchalsky and Curran, 1965). There are six independent parameters in three dimensional, where the real eigenvalues are the principle permeability, correspondingly the vectors are the principle flow directions.

Seepage in rock without any fractures is mainly controlled by the porosity n --the ratio between void volume V_v and total volume V.

$$n=\frac{V_v}{V} \tag{2.8}$$

Preprints (www.preprints.org) | NOT PEER-REVIEWED | Posted: 22 May 2018 doi:10.20944/preprints201805.0282.v1

The volume of specimen would be changed under forces, inducing the spatial parameter n would vary in the meanwhile. Therefore, the initial porosity would be n_0. Combining the Jacobian determinant $J=\frac{V}{V_0}$, an equation would be deduced (Borja and Alarcon, 1995).

$$J=\frac{1-n_0}{1-n} \tag{2.9}$$

The continuity equation governs the balance of the mass of a fluid flowing in a porous medium with absolute velocity $\mathbf{v}_f$. For a fully saturated medium, S_r=1, the continuity equation in a spatial form reads

$$\frac{\partial\left(nS_r\rho_f\right)}{\partial t}+div\left(n\rho_f v_f\right)=0 \tag{2.10}$$

which could be simplified as

$$\frac{\partial\left(Jn\right)}{\partial t}+div\left(Q\right)=0 \tag{2.11}$$

(Borja and Alarcon, 1995)

2.3. Mechanical equilibrium

Mechanical equilibrium requires that

$$\nabla\cdot\boldsymbol{\sigma}+\mathbf{f}=\mathbf{0} \tag{2.12}$$

σ is the total stress, which is contained by two parts- fluid and solid. $\mathbf{f}$ is material body force. According to Terzaghi's principle of effective stress, the total stress could be decomposed as

$$\boldsymbol{\sigma}=\boldsymbol{\sigma}'+\boldsymbol{\mu} \tag{2.13}$$

$$\sigma=\sigma'-p\mathbf{I} \tag{2.14}$$

σ' is effective stress and p is pore pressure. This equation denotes a relationship between fluid and solid, which is the basement in coupling. Therefore, the mechanical equilibrium and the Terzaghi's principle could deduce in polar coordinate

$$\frac{\partial\sigma_r'}{\partial r}+\frac{\sigma_r'-\sigma_\theta'}{r}=\frac{\partial\mu}{\partial r'} \tag{2.15}$$

σ_r' and σ_θ' are the radial and azimuthal components of the effective stress.

2.4. Constitutive laws

Constitutive laws determine the relationship among stress，strain and displacement. Phases of materials would have great influence in constitutive laws for the significant different properties in solid and fluid phases. As for the solid part, we hypothesize that the deformation is determined in an infinite elastic material subjected to in-situ stresses, and the material is assumed to be linearly elastic, perfectly plastic, with a failure surface defined by the Mohr-Coulomb criterion.(Itasca Consulting Group, 2012) Small and large-scale yielding that surrounds the crack tip also attributes to the Mohr-Coulomb pressure sensitive material, supporting the selection that Mohr-Coulomb would be the most accurate constitution law in this model(Papanastasiou P, Atkinson C., 2006; Panos Papanastasiou, Euripides Papamichos and Colin Atkinson, 2016). As for the fluid part, the permeability law is much easier to ascertain. The Kozeny-Carman formula contributes an equation relating the porosity and permeability. Furthermore, the constitution of interface should be selected independently.

2.4.1. Mohr-Coulomb Model

Assuming the material is linear elastic, perfectly accordant with Hoek elasticity. Therefore, the equation of stress and strain is

Preprints (www.preprints.org) | NOT PEER-REVIEWED | Posted: 22 May 2018 doi:10.20944/preprints201805.0282.v1

$$\boldsymbol{\sigma} = \mathbf{E} : \boldsymbol{\varepsilon} \tag{2.16}$$

Based on the thick wall cylinder theory, the result is Lame equation

$$\sigma_r = \frac{a^2}{b^2 - a^2}\left(1 - \frac{b^2}{r^2}\right)p_i - \frac{b^2}{b^2 - a^2}\left(1 - \frac{a^2}{r^2}\right)p_0$$

$$\sigma_\theta = \frac{a^2}{b^2 - a^2}\left(1 + \frac{b^2}{r^2}\right)p_i - \frac{b^2}{b^2 - a^2}\left(1 + \frac{a^2}{r^2}\right)p_0 \tag{2.17}$$

$$\tau_{r\theta} = 0$$

p_i is the inner pressure and p_0 is the outer pressure, which is zero here.

However, linear elasticity is an idealized constitutive model in figuring out the infinitesimal deformations when the stress applied on the cell does not reach the material's strength

Furthermore, the Mohr-Coulomb yield criterion is an integral judgement describing the deterioration of rock mass. The formulation is in the following.

$$c = \tau + \sigma_n \tan\phi \tag{2.18}$$

2.4.2. Permeability

Water is a magical factor for its incredible effects in softening materials and particular characters in uniform force. Although the hypothesis is that deformations could be induced for the elastic material. This model is a hollow cylinder cut by fracture, producing an interface. The permeability should be discussed as two parts: one is permeability in porous media; another is permeability in single fracture.

As for the porous media, although displacement induced by the rearrangement of solid skeleton is really small compared to elastic deformation, porosity altering is non-negligible. Based on the Kozeny-Carman formula, the deformation-dependent permeability is related to the constant permeability. The Kozeny-Carman formula is

$$\mathrm{k} = c_0 \frac{n^3}{(1-n)^2 M_s^2} \tag{2.19}$$

Where k is permeability. c_0 is the coefficient relating to empirical geometry. M_s is specific surface area.

At the initial state, $n = n_0$, $\mathrm{k}_0 = c_0 \dfrac{n_0^{\,3}}{(1-n_0)^2 M_s^2}$ (2.20)

When $t > 0$, $\mathrm{k} = c_0 \dfrac{n^3}{(1-n)^2 M_s^2}$, (2.21)

k is deformation-dependent permeability.

Then the normalized Kozeny-Carman formula is,

$$k = k_0 \frac{(1-n_0)^2}{n_0^{\,3}} \frac{n^3}{(1-n)^2} \tag{2.22}$$

As for the permeability in single fracture, k could be described as $k = d^2/12$ deduced by Navier-Stokes equation, in which d is opening width of fracture. The interface in this model is an ideal plane without width and thickness, thus d is regarded as 1 here.

However, anisotropic deformation is corresponding to the anisotropic permeability, which is quite complicated that not only the inhomogeneous material but also the different fluid flow could have different.

2.4.3. Interface

Preprints (www.preprints.org) | NOT PEER-REVIEWED | Posted: 22 May 2018 doi:10.20944/preprints201805.0282.v1

Joint, fault or bedding planes in geologic medium is a natural interface, as mutation of layer that may control the whole deteriorate behavior of rock mass. Assuming that the broken behaviors obey Coulomb Sliding, that is, the bond is either intact or broken. The key parameters of interface are combined by friction, cohesion, normal stiffness k_n and shear stiffness k_s. If the pore pressure is greater on the condition that the stress is under compressive normal force, effective tension is no more exist in broken bond segment. Shear force is limited by Coulomb shear-strength criterion by the relation

$$F_{s\max} = cA + \tan\phi\left(F_n - pA\right) \tag{2.23}$$

c is the cohesion along the interface. ϕ is the friction angle of the interface surface. p is pore pressure. When shear force is more than the limitation, sliding is assumed to occur.

Besides, the effective normal stress on the joint might soar due to the shear displacement, according to the relation

$$\sigma_n := \sigma_n + \frac{|\mathrm{F}_s|_o - F_{s\max}}{AK_s}\tan\psi k_n \tag{2.24}$$

ψ is the dilation angle of the interface surface. $|\mathrm{F}_s|_o$ is the magnitude of shear force before the preceding correction is made. (Itasca Consulting Group, 2012)

2.5. Boundaries

The initial state of the specimen is that all the displacements and velocities are zero. The porosity $n = n_0$, $\sigma_r|_{t=0} = \sigma_\theta|_{t=0} = 0$.

To simulate the reservoir with high water head, we put a load on the upper plane and in the hole, as an equal force as the constant water head. Besides radial direction of circumference of model is confined, simulating the fracture is embedded in infinite ground. Therefore, a constant pressure is applied on the upper plane while the static water pressure is also applied in the hole of cylinder. The pore pressure is also ascertained when the external load is settled down. Assuming the pore pressure of the upper plane is equal to the water head while the fluid will flow outward radially along the radius in thick wall cylinder. However, when there is fracture with different permeability, the flow path will become complicated due to the interface. The pore pressure in interface may not be accordant with the pore pressure in rock specimen.

3. Simulation of an example

A simulation of saturated cylinder with fractures is designed to figure out hydraulic fracturing coupling with seepage field and mechanic field during the process. This discontinuity increase the complexity in calculation, which applies finite difference to acquire the stress and strain distribution. The research selected FLAC 3D[5.01] to simulate the tests, using the Lagrangian analysis of continua method to solve discontinuity problem.

3.1. Building a model

According to the Figure 1, a system of reference axes is selected, with orientation in the center of the cylinder at the bottom plane. The concentric circles are located in x-z plane, of which the outward radius is 50mm and the inward radius is 10mm (0.010m). Extrusion along Y axis from the x-z plane is 120mm (the height of the hollow cylinder is 0.120m.). The circumference is divided into 40 equally while the radius between the out circle and inner circle is divided into 10 at the ratio of 1.2. The height is also divided into 20 parts equally. We select parameters of sand stone to have the simulate test. All the parameters are giving in Table 1, referring to Morita (1992).

Table 1. Material constants used for the porous model.

Preprints (www.preprints.org) | NOT PEER-REVIEWED | Posted: 22 May 2018 doi:10.20944/preprints201805.0282.v1

Rock mass	E(GPa)	G(GPa)	K(GPa)	Cohesion (MPa)	Friction (°)	n	C(m/s)	Tension (MPa)	Kn(N/m)	Ks(N/m)
rock	23	10	12	16	41.9	0.01	1.4e-14	12	/	/
interface	/	/	/	5	15	/	1.0e-12	/	2e8	2e8

*E: Elasticity modulus G: Shear modulus K: Bulk modulus C: Permeability coefficient.

The oblique plane cuts the hollow cylinder at certain angles, simulating different occurrences of fractures in rock mass. We set several models with different fracture angles and water pressure to mimic behaviors of varies. The angles of fractures are 0°, 15°, 30° and 45°.

The initial state is balanced first at the service of adding external loading. To figure out the fault activation effected by the value of water head and pore pressure, normal stress is applied on the plane distributed equally, regarding as water pressure. Exploration in relationship between water head and the displacement is needed in this simulation, changing the water head gradually, which are 50m, 100m, 150m, 200m, 250m and 300m. Numerical tests had been carried out to confirm that this increase of loading rate has very little influence on the material behavior of the sample. (Sousani Marina, Eshiet Kenneth Imo-Imo, Ingham Derek, 2014) Therefore, the increasing rate of water pressure is not set in this numerical test.

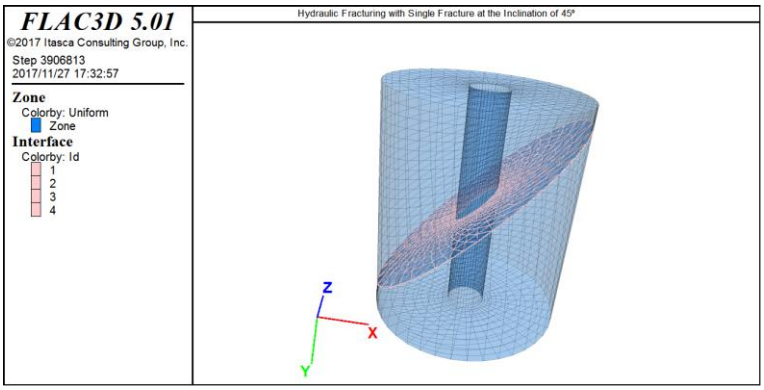

Figure 4. Contour of model with mesh and interface.

Since the fluid phase is existing in the saturated specimen, seepage field is a significant factor that should be coupled into this simulation. Assuming the cylinder is at the bottom of a reservoir, pore pressure is the same as the water pressure without considering the geotectonic stress. Besides, we hypothesize that the cylinder is embed in infinite space, which means the periphery of the cylinder is confined in x-z plane while the deformation of y axis is free.

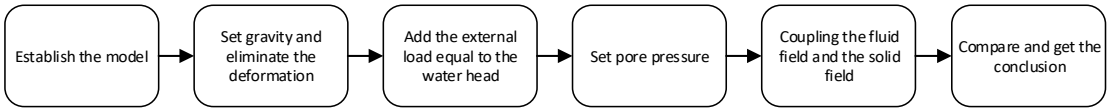

Figure 5. Process of simulating hydraulic fracturing.

3.2. Results and discussion

After all the models are calculated, displacements of certain points near the interface are recorded to demonstrate the deformation of holly cylinder. Furthermore, the stress and strain distribution could imply the mechanism of the deterioration inside the specimen. We selected two groups of points in each model. Three points are contained in each group perpendicular to the x-z plane, locating in a line at the same distance. The coordinates are listed in Table 2.

Preprints (www.preprints.org) | NOT PEER-REVIEWED | Posted: 22 May 2018 doi:10.20944/preprints201805.0282.v1

Table 2. Coordinate of selected points.

Inclination	0º	15º	30º	45º
Inner circle	(0.010 0.057 0)	(0.010 0.054 0)	(0.010 0.051 0)	(0.010 0.048 0)
	(0.010 0.060 0)	(0.010 0.057 0)	(0.010 0.054 0)	(0.010 0.051 0)
	(0.010 0.063 0)	(0.010 0.060 0)	(0.010 0.057 0)	(0.010 0.054 0)
Outer circle	(0.050 0.057 0)	(0.050 0.044 0)	(0.050 0.028 0)	(0.050 0.007 0)
	(0.050 0.060 0)	(0.050 0.047 0)	(0.050 0.031 0)	(0.050 0.010 0)
	(0.050 0.063 0)	(0.050 0.050 0)	(0.050 0.034 0)	013 0)

*The coordinates with underline means the point is in on the interface. Differences of displacement between points above or beneath the interface are recorded in mechanic field and coupling the solid phase and fluid phase.

Thus the difference of displacement between the two points above the interface and beneath the interface would imply disturbance and discontinuity of the specimen. For the convenience of contrast the displacement of point, 'series up' is defined as subtraction between upper grid and interface grid while 'series down' defined as subtraction between lower grid and interface grid. Subtraction of 'series up' and 'series down' could supply a relative location between hanging wall and foot wall of the fault. Based on this, 8 lines are drawn in one coordinate system.

To demonstrate problems explicitly, we first use a homogeneous model without considering any fractures and interfaces in hollow cylinder. Apparently, the deformation of homogeneous media is consistent. The results are in the following.

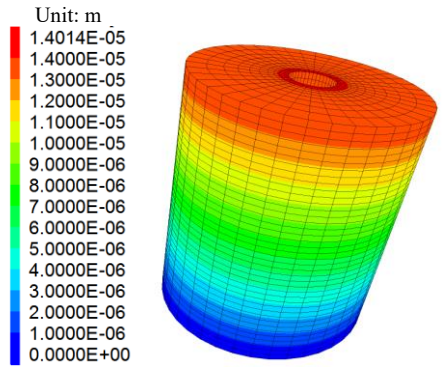

(1)Contour of displacement in mechanic field

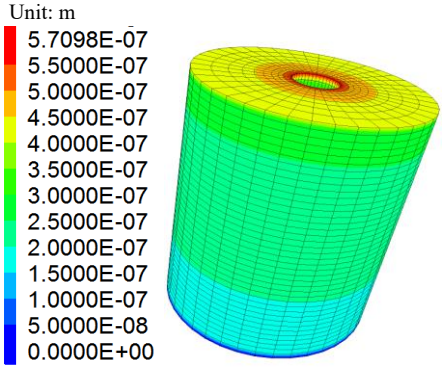

(2) Contour of displacement in coupling fields

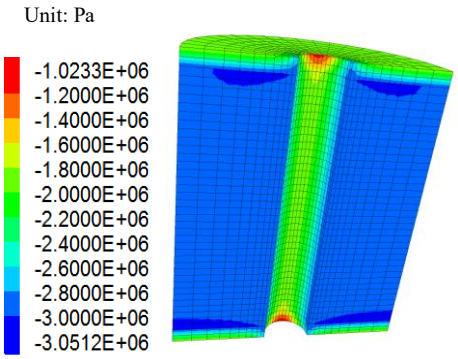

(3) a XX stress

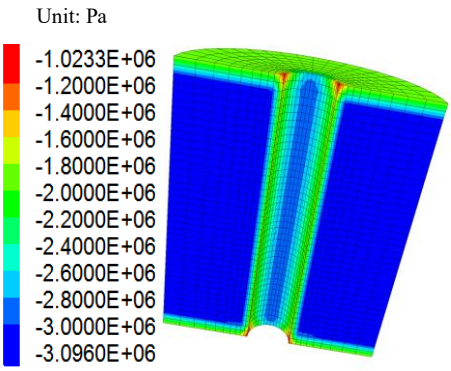

b ZZ stress

Preprints (www.preprints.org) | NOT PEER-REVIEWED | Posted: 22 May 2018 doi:10.20944/preprints201805.0282.v1

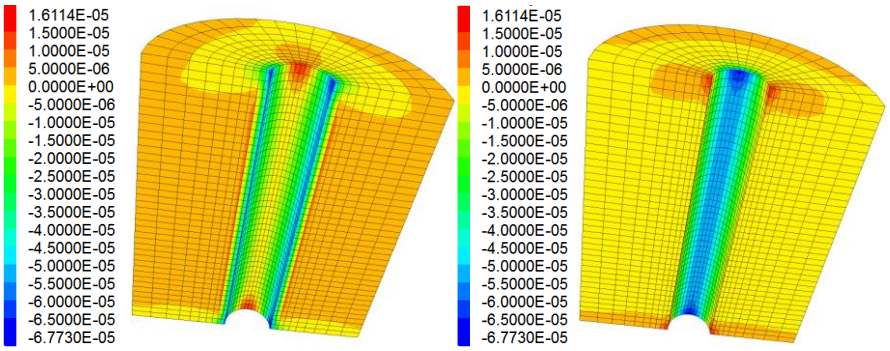

(4) a XX strain b ZZ strain

Figure 6. Contours in homogeneous thick wall cylinder without any fractures (transparent 50%), applied 3MPa pressure on upper plane of this model and subsequently added pore pressure to the specimen. Picture (1) is a contour of displacement solved only on the condition of mechanic field, without considering Terzaghi's principle. Picture (2) is resolved by coupling the solid phase and fluid phase, which significantly improves that pore pressure is not a negligible factor in analyzing problems relating to rock mass.

Since the model is asymmetric, stress and strain distribute almost the same in symmetric direction. The positive means the stress and strain compressive pressure. Correspondingly, negative means tension. Sand stone is relatively hard rock, uneasy to break up while the loading less than its strength, till in the elastic process. The difference of displacement of points is almost 0 for the continuity.

Then models with different interfaces are introduced to evaluate effects given by inclination of faults. External loading is added equilibrium to the water pressure on the upper plane of cylinder and in the hole, only considering the mechanic field without setting pore pressure in rock. The curves are exhibited in the following.

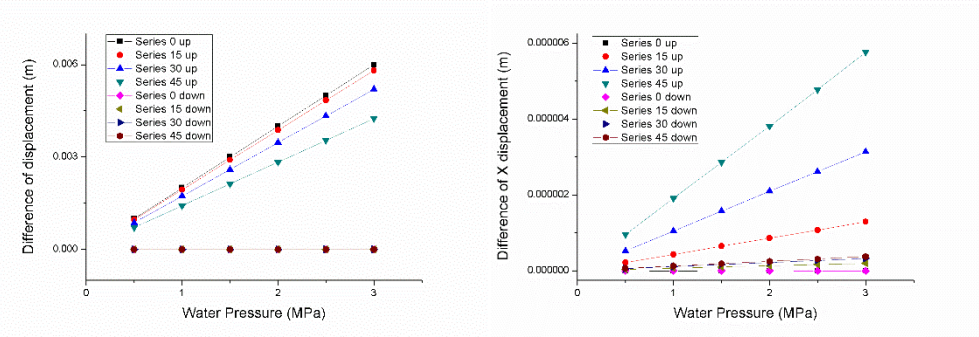

(1) Δdisplacement of inner circle (2) ΔX of inner circle

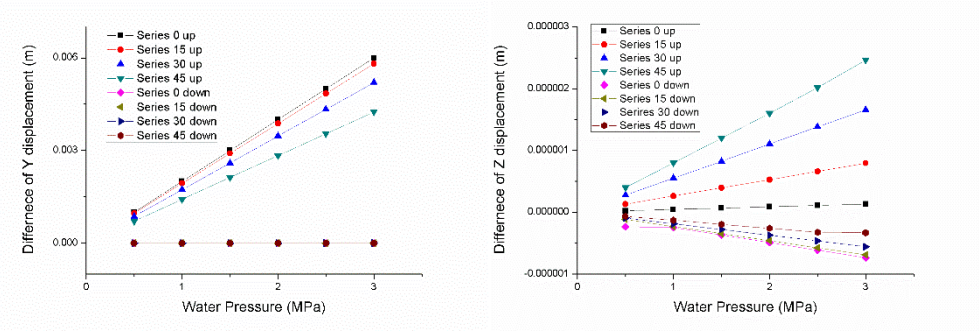

(3) ΔY of inner circle (4) ΔZ of inner circle

Preprints (www.preprints.org) | NOT PEER-REVIEWED | Posted: 22 May 2018 doi:10.20944/preprints201805.0282.v1

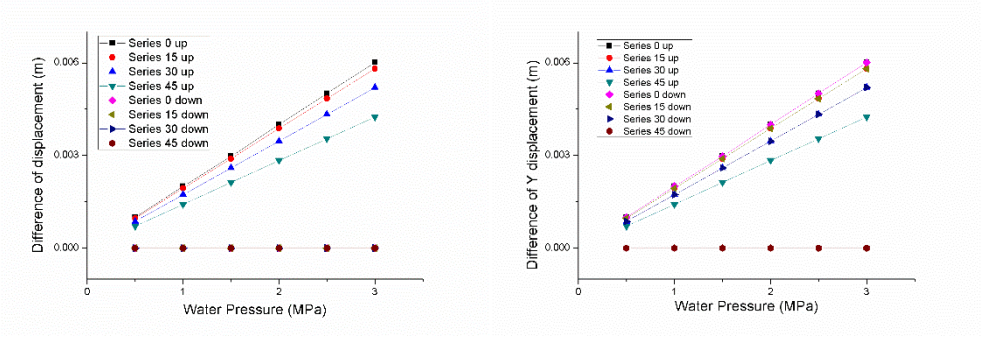

(5) ΔDisplacement of outer circle (6) ΔY of outer circle

Figure 7. Difference of displacements acquired by only simulating the single fracture model with equilibrium water pressure, without considering the pore pressure and seepage field inside the specimen.

These curves are quite special that difference of displacement and Y are descending while the inclination of interface is increasing. Besides the slope of different models attenuates much rapidly as the inclination of single fracture ascend gradually by a step of 15° On the contrary, ΔX and ΔZ are rising. This phenomenon may be caused by creating micro fissures.

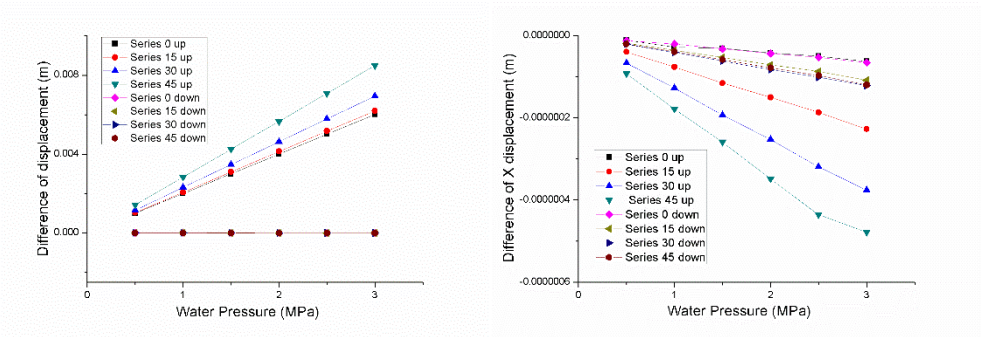

(1) Δ Displacement of inner circle (2) Δ X of inner circle

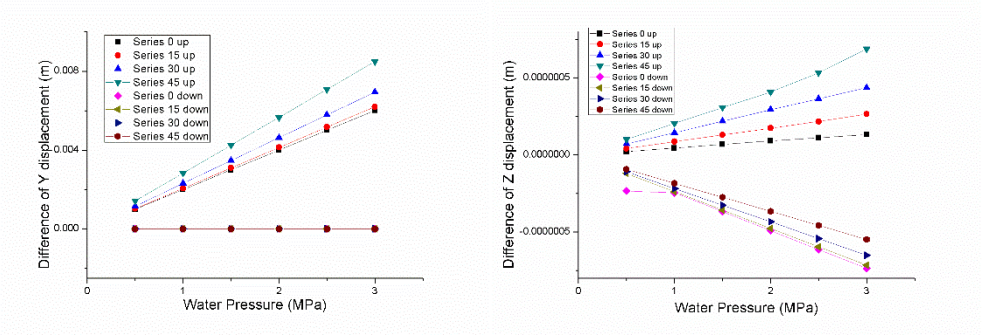

(3) ΔY of inner circle (4) ΔZ of inner circle

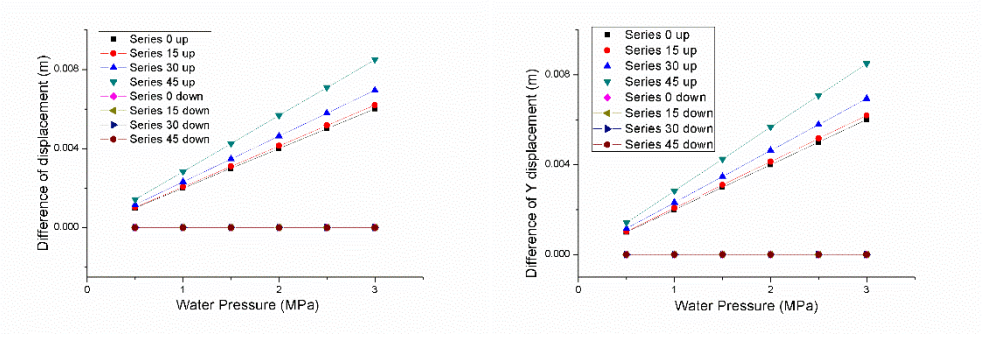

(5) Δ Displacement of outer circle (6) ΔY of outer circle

Figure 8. Difference of displacements acquired by coupling solid phase and fluid phase.

According to figure 8, the differences of displacement between outer circle and inner circle imply that movement of rock mass above the interface is much more than that beneath the interface. Discontinuity in z direction could generate a slight fissure inside this cylinder. Besides, with the increase of inclination, the difference of rock mass on the either side of the fracture also grows gradually. Up planes of this fault could be activated due to the discontinuity in x axis. What's more, the cylinder with interface inclination at 0 cannot be regarded as two integral thick-wall cylinder attached together because the x and z displacement of cells are supposed to be zero if the specimen is homogeneous. There might be a micro fissure propagating near the interface while the water is injected into the hole for the soft layer or structure plane embedded in two layers.

Therefore some rules could be concluded that the displacement increases linearly with the water pressure and inclination of interface. The deformation of each point is mainly determined by the displacement along y axis, which could be counted as millimeters in spite that the height of model is 120mm, although the displacement under the interface can be neglected. This data implies that the deformation of this specimen is discontinues for the existence of interface, which can absorb energy in the form of sliding and condensing.

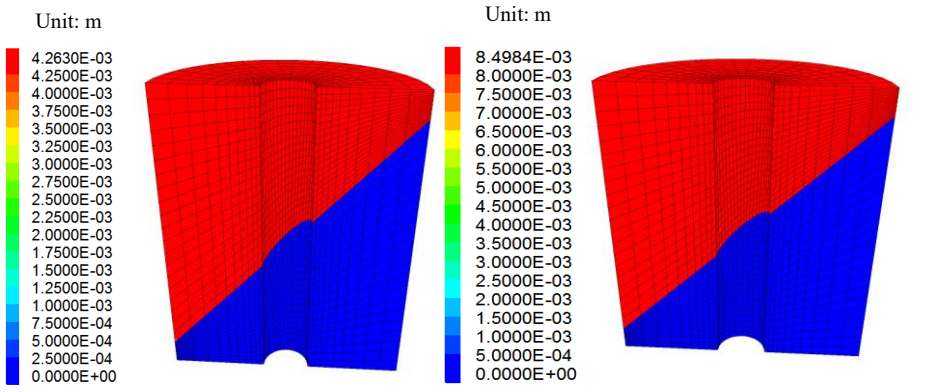

(1)Contour of displacement in mechanic field (2) Contour of displacement in coupling fields

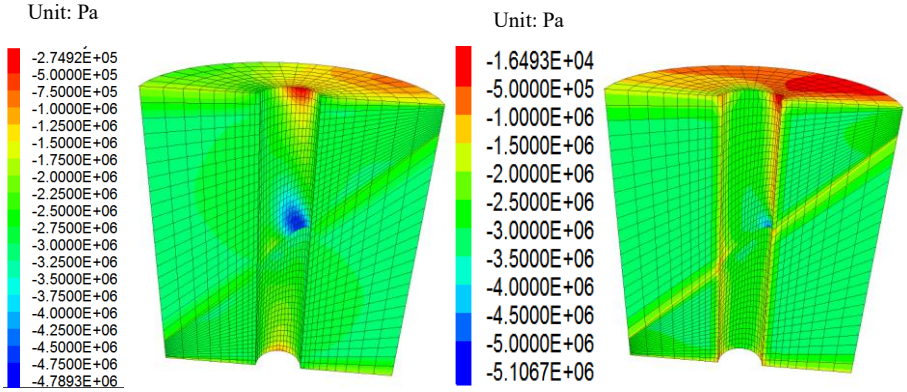

(3) a XX stress b ZZ stress

Preprints (www.preprints.org) | NOT PEER-REVIEWED | Posted: 22 May 2018 doi:10.20944/preprints201805.0282.v1

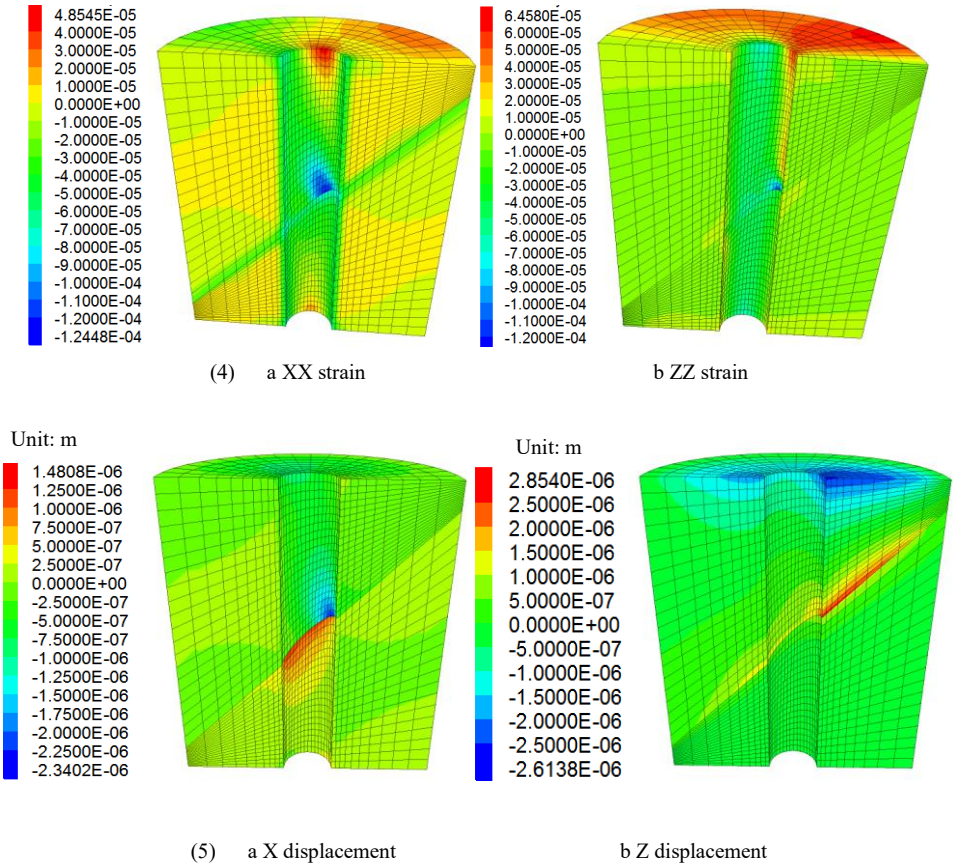

Figure 9. Contours half hollow cylinder with single fracture at the angle of 45°, applied 3MPa pressure on upper plane of this model. The stress and strain distribution coupling fluid phase is not asymmetric since the single fracture changes the particular character. Stress and strain alters significantly along the long axis of this interface.

To verify the opinions above, contours of X-displacement and Z-displacement (Figure 9.) shows that cracks might generate and propagate near the hole after injecting water. But the most crucial factor is water pressure, applied long the y direction, controlling the value and direction of principle stress, triggering the sliding of the fault. Micro cracks may create and propagate long X axis for the stress concentration. Subsequently, movement of interface could release energy inside the rock mass, and induce seismicity.

Comparing the data only calculated the mechanic field and coupling the fluid phase, a conclusion could be acquired that the characteristics of displacements of rock mass is quite different for the effective stress principle. Pore pressure could eliminate the effective stress essentially and increase the displacement difference between the higher plate and lower plate of a fault.

Based on the results above, these data implies that the water pressure and the inclination of single fracture can really influence the characters of mechanic behaviors, which is a significant signal indicating people could evaluate the stability of a reservoir. The simulation result implies that the displacement line would get steeper with the crack angle. Therefore monitoring the data of displacement would offer the exact description of the interface.

The mechanism of this model could be described that the primary fracture or fault could change the response under the same boundary condition. Cracks will not generate and propagate as the same prediction as the practical tests and numerical simulations experimented in thick-wall cylinder. Hydraulic pressure can mainly activate faults because the displacements in y direction could be 1000 times than displacements in x and z direction. Discontinues medium makes mechanic field become much complexing, leading to stress concentration near the fault, which is a basic reason why the fault could be damaged and release the energy. Furthermore, energy released in the fault could be changed into dynamic excitation. To be more specifically, an induced seismicity could be created after water

injected into the model. A relation between the parameters of a dynamic excitation and the energy released from the amplitude and frequency of the seismicity should be established by counting the displacements and stress of every cell.

4. Conclusion

Hollow cylinder cut by single fracture is discussed in this model, applied water pressure on the up plane and in the hole while pore pressure is set after solving the mechanic problem, which is coupling solid phase and fluid phase. According to the simulation, displacement is linearly increasing with the water pressure in the same model. Differences of displacement between the high plate and lower plate is decreasing when the inclination of single fracture increase under the same water pressure, only considering mechanic field. On the contrary, differences of displacement will increase with the inclination rise after coupling fluid phase, indicating the significant influence offered by Terzaghi's effective principle. Stress and strain distribution changes for the interface, because the discontinuity alter plane strain problem into three dimensional deformation. The most particular characteristic of asymmetry is totally broken up in spite that the fracture is parallel to up plane, exceeding common knowledge that the mechanic behavior would be similar to homogeneous cylinder. Comparing displacement in thick-wall cylinder and model with single fracture, fault could be damaged compressive force offered by water pressure, thus energy could be released by deformation and triggering activation of fault. These inspires people that deformation of rock mass could be evaluated while impounding a reservoir for the linear rule between deformation and water pressure. And hydraulic fracturing in wells utilized in exploration of shale gas should avoid fractures since the ability of creating and propagating cracks would attenuate obviously based on this simulation. Further study on how the seismicity effect the primary faults and creating new cracks should be studied. This relation could predict other factor while monitoring some of these, deducing where and how the seismicity come and act on the rock mass, deteriorating it and generating new cracks.

Acknowledgement

The authors would acknowledge Dr. Guan, Dr. Du and Dr. Xu for providing good suggestions in plotting figures. They gave us brilliant ideas in making the pictures looking more beautiful.

Funding: This work was supported by the National Natural Science Foundation-Outstanding Youth Foundation (grant number 51522903), the National Natural Science Foundation of China (grant numbers 41772246, U1361103, 51479094), the State Key Laboratory of Hydro-science and Engineering (grant numbers 2016-KY-02, 2016-KY-04, 2016-KY-05).

Reference

[1] Ameen, M.S., 2014. Fracture and in-situ stress patterns and impact on performance in the Khuff structural prospects, eastern offshore Saudi Arabia. Mar. Pet.. Geol. 50, 166-184. DOI: 10.1016/j.marpetgeo.2013.10.004

[2] Beekman, F., Badsi, M., Wees, J.D.V., 2000. Faulting, fracturing and in situ stress prediction in the Ahnet Basin, Algeria - a finite element approach. Tectonophysics 320, 311-329.

[3] Biot, M. , 1972. Theory of finite deformations of pourous solids. Indiana Univ. Math. J. 21, 597–620 .

[4] Bjerrum, L. and Andersen, K.H. 1972. In-situ Measurement of Lateral Pressures in Clay. Proc. of the 5th European Regional Conference on SMFE, Madrid, Spain, Vol.1,

[5] Borja, R.I. , Alarcon, E. , 1995. A mathematical framework for finite strain elastoplastic consolidation. part 1: balance laws, variational formulation, and linearization. Comput. Methods Appl Mech Eng 122, 145–171 .

[6] Brudy, M., Zoback, M.D., 1999. Drilling-induced tensile wall-fractures: implications for determination of in-situ stress orientation and magnitude. Int. J. Rock Mech. Min. 36, 191-215.

[7] Charlez, P., Despax, D., 1985. The state of stress in the earth crust: its importance in petroleum engineering.

14th Annual Convention Proceedings, Indonesian Petroleum Association. 2, 299-308.

[8] Chen, W., Ravichandran, G., 1996. An experimental technique for imposing dynamic multiaxial compression with mechanical confinement, Exp. Mech. 36 (2), 155–158.

[9] Cleary, M. P., Wong, S. K., 1985, Numerical simulation of unsteady fluid flow and propagation of a circular hydraulic fracture. Int. J. Numer. Anal. Met. 9, 1-14

[10] Decker, R. A. and Clemence, S. P., 1981. Laboratory Study of Hydraulic Fracturing in Clay. Proc of The 10th IESMFE, Stockholm, Sweden, Vol. 1, 573~575

[11] Itasca Consulting Group, 2012. Fast Lagrangian Analysis of Continua in 3 Dimensions Manual. Theory and Background.

[12] Gomberg J, Bodin P, Larson K, Dragert H, 2004. Earthquake nucleation by transient deformations caused by the M = 7.9 Denali, Alaska, earthquake. Nature 427:621–624

[13] Huang Wen-xi, 1982. Some comments on research works related to rock-fill dam. Water Resources Hydropower Engineering, 4: 23—27.

[14] Jaeger, J.C., Cook, N.G.W., 1979. Science Paperbacks. Fundamentals of rock mechanics, third ed., 9, pp. 251-252

[15] Johnson PA, Carpenter B, Knuth M, Kaproth BM, Le Bas PY, Daub EG, Marone C, 2012. Nonlinear dynamic triggering of slow slip on simulated earthquake faults with implications to Earth. J Geophys Res 117, B04310

[16] Kachanov M, Prioul R, Jocker J., 2010. Incremental linear-elastic response of rocks containing multiple rough fractures: similarities and differences with tractionfree cracks. Geophysics. 75(1), D1–11.

[17] Katchalsky, A.K. , Curran, P.F. , 1965. Nonequilibrium Thermodynamics in Biophysics. Harvard University Press .

[18] Kennett B., 2009.Seismic wave propagation in stratified media. Australia: National University E Press, Canberra; p. 288.

[19] Kim, J., Moridis, G.J., 2015. Numerical analysis of fracture propagation during hydraulic fracturing operations in shale gas systems. Int. J. Rock Mech. Min. 76, 127-137.

[20] Kranz, R.L. , 1983. Microcracks in rocks: a review. Tectonophysics 100 (1), 449–480.

[21] L. C. Auton, C. W., 2017. MacMinn, Fron arteries to boreholes: steady-state response of a poroelastic cylinder to fluid injection. Proc Math Phys Eng Sci. 473, 1-19. DOI: 10.1098/rspa.2016.0753.

[22] Li, H., Wong, L.N.Y., 2012. Influence of flaw inclination angle and loading condition on crack initiation and propagation. Int. J. Solids Struct. 49, 2482-2499.

[23] Maria Laura De Bellis, Gabriele Della Vecchia, Michael Ortiz, Anna Pandolfib, 2017. A multiscale model of distributed fracture and permeability in solids in all-round compression. Journal of the Mechanics and Physics of Solids. 104, 12-31.

[24] Moes, N., Dolbow, J., Belytschko, T., 1999. A finite element method for crack growth without remesing. Int. J. Numer. Meth. Eng. 46, 131-150.

[25] Morita, N., Gray, K.E., Sroujl, F.A .A ., Jogi, P.N., 1992. Rock-property changes during reservoir compaction. Soc. Petrol. Eng. Formation Eval. 7 (3), 197–205. DOI: 10.2118/13099-PA .

[26] Nagy PB, 1992. Ultrasonic classification of imperfect interfaces. J Nondestruct Eval. 11(3/4), 127–39.

[27] Nelson, E.J., 2005. Transverse drilling-induced tensile fractures in the West Tuna area, Gippsland Basin, Australia: implications for the in situ stress regime. Int. J. Rock Mech. Min. Sci. 42, 361-371.

[28] Nobari, E. S. , Lee, K. L. and Duncan, J. M., 1973. Hydraulic Fracturing in Zoned Earth and Rockfill Dams. Report No. TE-73-1, College of Engineering Office of Research Service, University of California, Berkley, California,

[29] P. Grassl, C. Fahy, D. Gallipoli, S.J. Wheeler, 2015. On a 2D hydro-mechanical lattice approach for modelling hydraulic fracture. Journal of the Mechanics and Physics of Solids. 75, 104-118.

[30] Panos Papanastasiou, Euripides Papamichos and Colin Atkinson, 2016. On the risk of hydraulic fracturing in CO2 geological storage. International Journal for Numerical and Analytical Methods in Geomechanics. 40,1472-1484.

[31] Papanastasiou P, Atkinson C., 2006. Representation of crack-tip plasticity in pressure-sensitive geomaterials: large scale yielding. International Journal of Fracture. 139, 137–144.

[32] Saipeng Huang, Dameng Liu, Yanbin Yao, 2017. Natural fractures initiation and fracture type prediction in coal reservoir under different in-situ stresses during hydraulic fracturing. Journal of Natural Gas Science and Engineering. 43, 69-80.

[33] Sousani Marina, Eshiet Kenneth Imo-Imo, Ingham Derek, 2014. Pourkashanian Mohamed, Sheng Yong, Modelling of hydraulic fracturing process by coupled discrete element and fluid dynamic methods. Environment Earth Science. 72, 3383-3399.

[34] Spencer TW, Edwards CM, Sonnad JR, 1977. Seismic wave attenuation in nonresolvable cyclic stratification. Geophysics. 42(5), 939–49.

[35] Voisin C, Campillo M, Ionescu IR, Cotton F, Scotti O, 2000. Dynamic versus static stress triggering and friction parameters: Interface from the November 23, 1980, Irpinia earthquake. J Geophys Res. 105, 21647–21659.

[36] W. Wu, J. Zhao, 2014. A Dynamic-induced Direct-shear Model for Dynamic Triggering of Frictional Slip on Simulated Granular Gouges. Experimental Mechanics. 54, 605-613

[37] Wei Wu, Haibo Li, Jian Zhao, 2015. Dynamic responses of non-welded and welded rock fractures and implication for P-wace attenuation in a rock mass. International Journal of Rock Mechanics & Mining Sciences. 77, 174-181.

[38] Wei Wu, Zhihong Zhao, Kang Duan, 2017. Unloading-induced instability of a simulated granular fault and implications for excavation-induced seismicity. Tunnelling and Underground Space Technology. 63, 154-161.

[39] Wong, R.H.C., Chau, K.T., Wang, P., 1996. Microcracking and grain size effect in yuen long marbles. Int. J. Rock Mech. Min. Sci. 33 (5), 479–485.

[40] Xiaoxi Men, Chunan Tang, Tianhui Ma, 2014. Numerical Simulation on Influence of Rockmass Parameters on Fracture Propagation During Hydraulic Fracturing. Journal of Northeastern University (Natural Science). 34(5), 700-703.

[41] Yao, Y., 2012. Linear elastic and cohesive fracture analysis to model hydraulic fracture in brittle and ductile rocks. Rock Mech. Rock Eng. 45, 375-387.

[42] Yaping Sun, 1985. Study on Mechanism of Hydraulic Fracturing. Tsinghua university, Beijing.

[43] Zhang Hui, 2005. Experimental Study and numerical simulation of hydraulic fracturing in core of rockfill dam. Hohai University, Nanjing.